TABLE OF CONTENTS

APPENDIX FIGURE LEGENDS

Appendix Figure S1. Reciprocal IP confirmed AMBRA1-VIF interaction

N-terminally or C-terminally FLAG-tagged AMBRA1 and empty vector or Strep-tagged HIV-1 constructs were co-transfected in HEK293T cells and subjected to FLAG IP. IP and input lysates were analyzed by immunoblot. Asterisk denotes non-specific bands.

Appendix Figure S2. AMBRA1 depletion enhances HIV-1 infectivity

Similar to Figure 2, human primary CD4+ T cells with *AMBRA1* knockout using Cas9 RNPs were infected with HIV-1 NL4-3 IRES-GFP reporter virus that resulted in 2% infectivity in the NT cells. Infectivity was measured by flow cytometry 48 h post-infection. Pair-wise comparisons between NT and the gene of interest were carried out by Mann-Whitney-Wilcoxon Test (**p*-value < 0.05). Bar graph represents mean + SEM, n=3.

Appendix Figure S3. AMBRA1-knockout HEK293T cells generated with the CRISPR-Cas9 system

A Cartoon depicts the AMBRA1 sgRNA-targeting region. Red, sgRNA sequence; blue, the PAM.

B HEK293T cells transfected with the AMBRA1 sgRNA-encoding plasmid (cloned into SpCas9-P2A-GFP, Addgene #48138) for 48–72 h were FACS-sorted into tubes based on GFP expression. Expanded polyclonal AMBRA1 knockout (KO) and parental HEK293T cells were analyzed by immunoblot.

C Alignment of the sequence reads from parental and AMBRA1 KO #4 HEK293T cells (clonally selected from AMBRA1 sgRNA–transfected HEK293T cells) encompassing

human AMBRA1 exon2. "-" denotes deletion of nucleotides. Of note, AMBRA1 KO #2 cells (also edited with the same AMBRA1 sgRNA) may contain a large insertion/deletion that could not be amplified with the same set of PCR primers.

Appendix Figure S4. APOBEC3G degradation by $CRL5^{VIF}$ is upregulated in an AMBRA1-depleted background

A, B Co-expression of HA-tagged APOBEC3G (A3G), increasing amounts of Strep-tagged VIF, and transfection control GFP in parental HEK293T, AMBRA1 knockout (KO) cells #2 (A) or KO #4 (B). The total amount of transfected DNA was kept constant by adding empty vector. Lysates were analyzed by immunoblot. Asterisk denotes non-specific bands.

C Similar to described in (B), but included empty vector control or re-expression of AMBRA1 in AMBRA1 KO #4 background.

D Similar co-transfection experiment was carried out with empty vector control, FLAG-ELOC, or co-expression of FLAG-ELOC and FLAG-ELOB.

Appendix Figure S5. Removal of predicted N-terminal helical region of AMBRA1 resulted in both gain and loss of protein-protein interactions

A Predicted secondary and tertiary structures of AMBRA1. Upper panel depicts alignment of AMBRA1 N-terminal sequence with other DCAFs (Robert & Gouet, 2014). The structure of DDB2 in complex with DDB1 was used as a template to represent the conserved motif (PDB ID: 3EI4). Lower panel shows a homology model of the AMBRA1 N-terminal region encompassing a helical region important for DDB1 binding and a partial WD40 domain, generated by SWISS-MODEL using human DNA excision repair protein ERCC-8 (CSA/ERCC8) as a template (Biasini *et*

al, 2014). Red colored residues denote breakpoints for generating ΔH22, ΔH34, and ΔH43 AMBRA1 mutants.

B Volcano plot showing gain (red) and loss (blue) of interactions by ΔH22 mutant versus WT AMBRA1 in three independent AP-MS experiments (also see Figure 3C).

C, D Bar graphs showing the abundance of purified/co-purified proteins with (C) and without (D) VIF expression, represented by integrated peak intensity from the parental-ion mass analysis using MaxQuant. Statistical analysis of paired comparison was carried out using MSstats (Choi *et al*, 2014) (*p*-values * < 0.05; ** < 0.01; **** < 0.0001; n.s. not significant). Note that CUL4A was not detected in ΔH43 AP-MS in the presence of VIF (C).

Appendix Figure S6. Binding specificity of AMBRA1 for ELOC and not SKP1

A Alignment of ELOC and SKP1 amino acid sequences.

B Parental or stable HEK293T cells expressing FLAG-tagged ELOC or SKP1 were purified with anti-FLAG beads. IP and input lysates were examined by immunoblot.

Appendix Figure S7. Mapping AMBRA1 and ELOC interacting regions

A WT AMBRA1 and its deletion mutants were expressed in HEK293T cells, followed by lysis and IP.

B Scheme of the AMBRA1 deletion constructs used in (A). The ability of these mutants to interact with DDB1 is annotated by + and – signs.

C WT ELOC and the 1–90 mutant were expressed in HEK293T cells and were immunoprecipitated using anti-FLAG beads. The input lysate and IP samples were analyzed by immunoblot. EV stands for empty vector and FL stands for full-length ELOC (amino acids 1–112).

Appendix Figure S8. ELOC, not ELOB, shows MG132- and ubiquitin K48-dependent polyubiquitination

A HEK293T cells stably expressing FLAG-ELOB or FLAG-ELOC were transfected with myc-ubiquitin or empty vector, followed by DMSO or MG132 treatment and denaturing IP. IP and input lysates were examined by immunoblot.

B ELOC polyubiquitination is accumulated by proteasomal inhibition and reduced by K48R ubiquitin mutation. Denaturing IP of ELOC was performed on HEK293T cells stably expressing FLAG-ELOC transfected with WT or K48R myc-ubiquitin. Before harvested for IP, cells were treated with DMSO control or 5 μM MG132 for 6 hours. IP and input lysates were examined by immunoblot.

Appendix Figure S9. ELOC is a ubiquitination substrate targeted by $CRL4^{AMBRA1}$

FLAG-ELOC-expressing HEK293T cells were pre-treated with 10 nM of NT or AMBRA1 siRNA, followed by MG132 treatment and denaturing IP. IP and input lysates were examined by immunoblot.

Appendix Figure S10. AMBRA1 knockdown does not affect the mRNA expression of ELOB and ELOC

HEK293 cells stably expressing NT or the indicated AMBRA1 shRNA were measured for expression of *AMBRA1*, *ELOB*, and *ELOC* using qPCR. Relative mRNA expression was normalized against the house-keeping gene *GAPDH* and plotted in ratio relative to the NT control.

Appendix Figure S11. Confirmation of ATG- and CUL4A-knockout HEK293T clones

A, B CUL4A-knockout HEK293T cells were confirmed by the protein depletion via immunoblot (A) and genomic DNA PCR of the targeting region (B). Clone#36 was used in Figure 5D. Asterisks denote nonspecific bands.

C Functional validation of ATG7- and ATG12-knockout HEK293T cells. Lysates from control, ATG7-, and ATG12-knockout clonal HEK293T cells were analyzed by immunoblot. ATG7- and ATG12-knockout were verified by the protein depletion and the accumulation of p62/SQSTM as a result of autophagy deficiency.

D Genotyping data of the CRISPR-Cas9-mediated ATG-knockout cell lines used in this study. Red, single-chimeric guide RNA (sgRNA) sequences; blue, photospacer-associated motifs (PAMs). "-" denotes deletion of nucleotides; "*" indicates insertion of nucleotides (highlighted in bold italics).

Appendix Figure S12. VIF is stabilized by blocking its autocatalysis

Expression of VIF-GFP and VIF L145A-GFP in HEK293 cells was induced by the addition of 1 μg/mL dox for 16 hours, followed by the addition of 100 μg/mL of CHX at different time points. Lysates were analyzed by immunoblot.

Appendix Figure S13. Substrate-shielding effect

A Increased CBFβ polyubiquitination by VIF overexpression. HEK293T cells co-expressing FLAG-tagged CBFβ, myc-ubiquitin along with empty vector, or Strep-tagged VIF were affinity purified under denaturing conditions with anti-FLAG to examine ubiquitin incorporation into CBFβ. IP and input lysates were analyzed by immunoblot. Note that a trace amount of FLAG antibody light chain detected in the IP eluates masks Strep immunodetection.

B Model depicting substrate-shielding effect. VIF is sensitive to autoubiquitination in

the absence of its binding partner CBFβ and the VIF substrate APOBEC3.

APPENDIX REFERENCES

Biasini M, Bienert S, Waterhouse A, Arnold K, Studer G, Schmidt T, Kiefer F, Gallo Cassarino T, Bertoni M, Bordoli L, Schwede T (2014) SWISS-MODEL: modelling protein tertiary and quaternary structure using evolutionary information. *Nucleic Acids Res* 42: W252-8

Choi M, Chang C-Y, Clough T, Broudy D, Killeen T, MacLean B, Vitek O (2014) MSstats: an R package for statistical analysis of quantitative mass spectrometry-based proteomic experiments. *Bioinformatics* 30(17): 2524-2526

Robert X, Gouet P (2014) Deciphering key features in protein structures with the new ENDscript server. *Nucleic Acids Research* 42: W320-W324

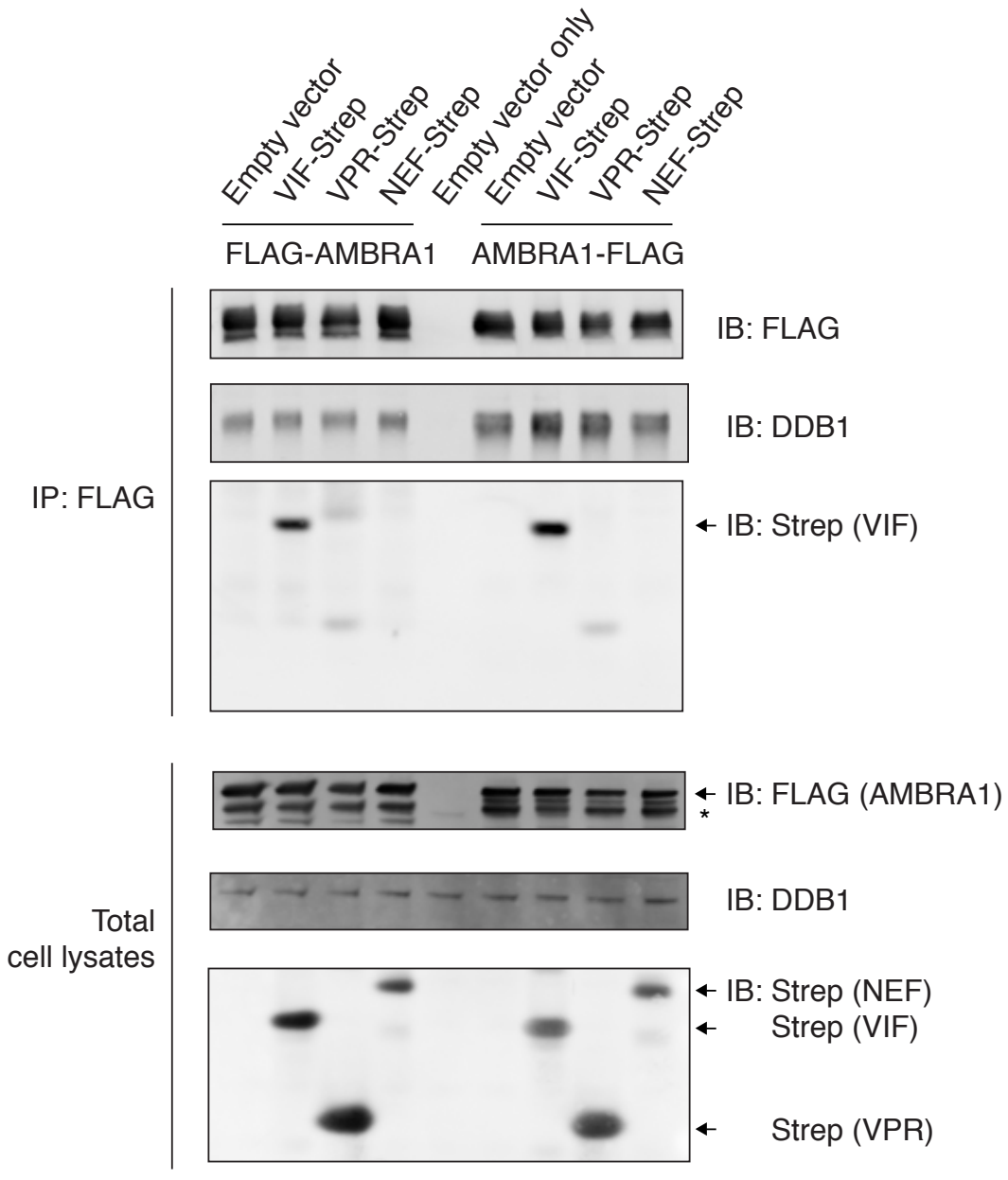

Chen SH et al., Appendix Figure S1

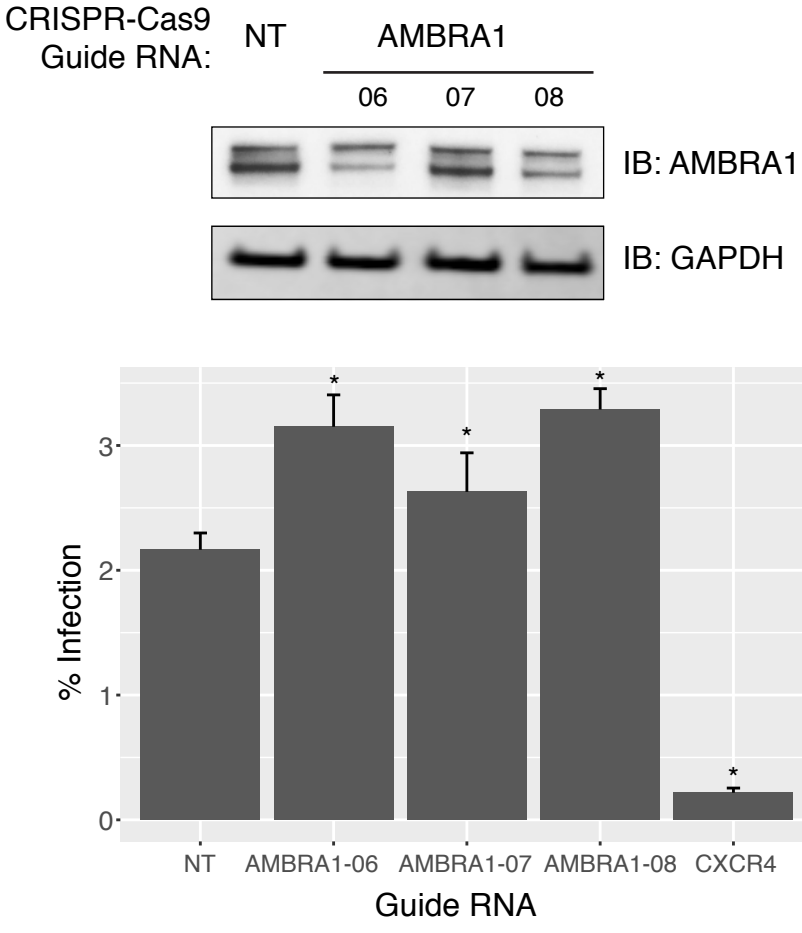

Chen SH et al., Appendix Figure S2

A

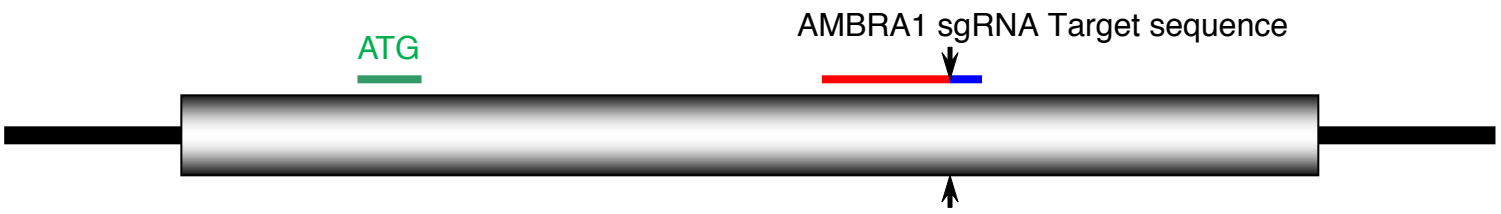

B

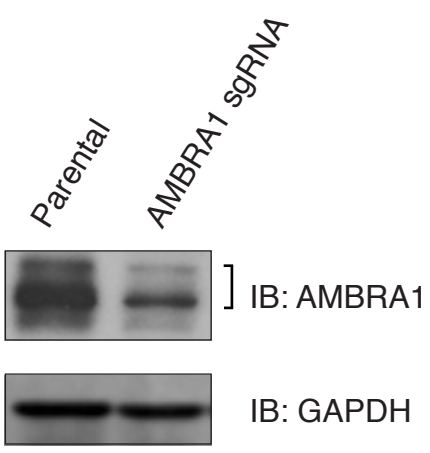

C

```
                                                                PAM
            WT: ATGGGAGCTCAGCGGCTTCTGCAGGAGCTGGTAGAAGATAAAACCCGGTGGATGAAATGGGAG
AMBRA1 KO#4-1: ATGGGAGCTCAGCGGCTTCTGCAGGAGC----------------CGGTGGATGAAATGGGAG
AMBRA1 KO#4-2: ATGGGAGCTCAGCGGCTTCTGCAGGAGC----------------CGGTGGATGAAATGGGAG
AMBRA1 KO#4-3: ATGGGAGCTCAGCGGCTTCTGCAGGAGC----------------CGGTGGATGAAATGGGAG
AMBRA1 KO#4-4: ATGGGAGCTCAGCGGCTTCTGCAGGAGCTGGTAGAAGATAAAACC-GGTGGATGAAATGGGAG
AMBRA1 KO#4-5: ATGGGAGCTCAGCGGCTTCTGCAGGAGCTGGTAGAAGATAAAACC-GGTGGATGAAATGGGAG
AMBRA1 KO#4-6: ATGGGAGCTCAGCGGCTTCTGCAGGAGCTGGTAGAAGATAAAACC-GGTGGATGAAATGGGAG
AMBRA1 KO#4-7: ATGGGAGCTCAGCGGCTTCTGCAGGAGCTGGTAGAAGATAAAACC-GGTGGATGAAATGGGAG
AMBRA1 KO#4-8: ATGGGAGCTCAGCGGCTTCTGCAGGAGCTGGTAGAAGATAAAACC-GGTGGATGAAATGGGAG
```

Chen SH et al., Appendix Figure S3

A

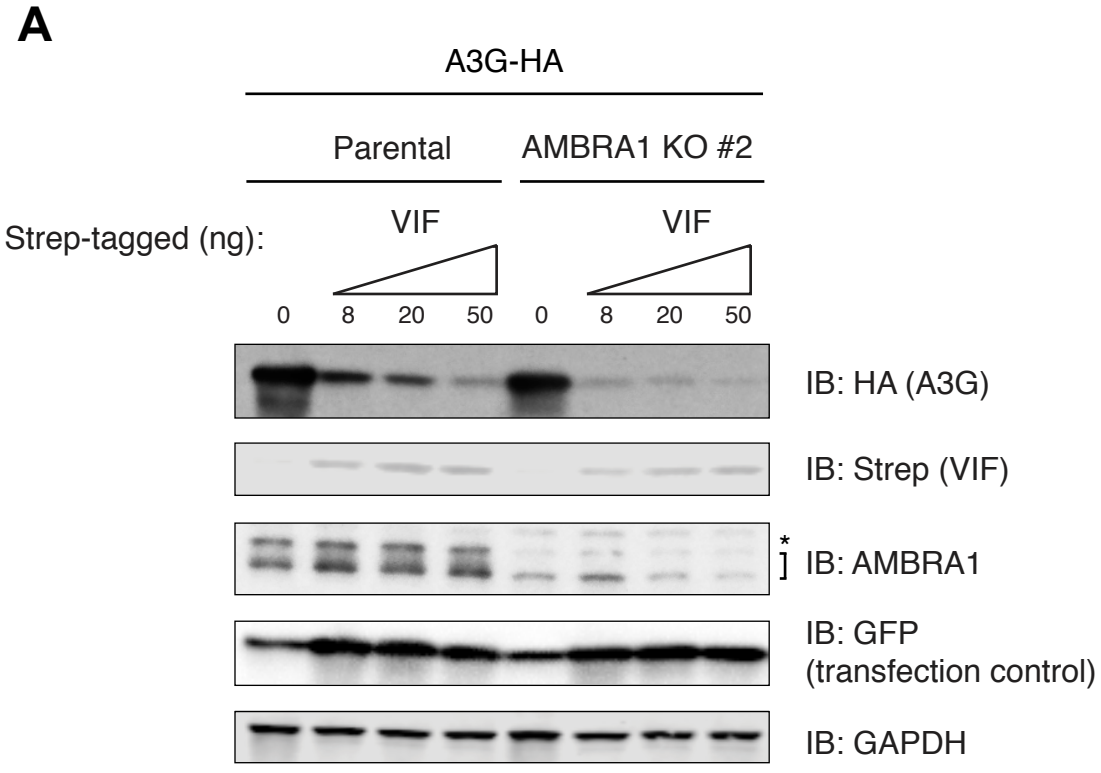

B

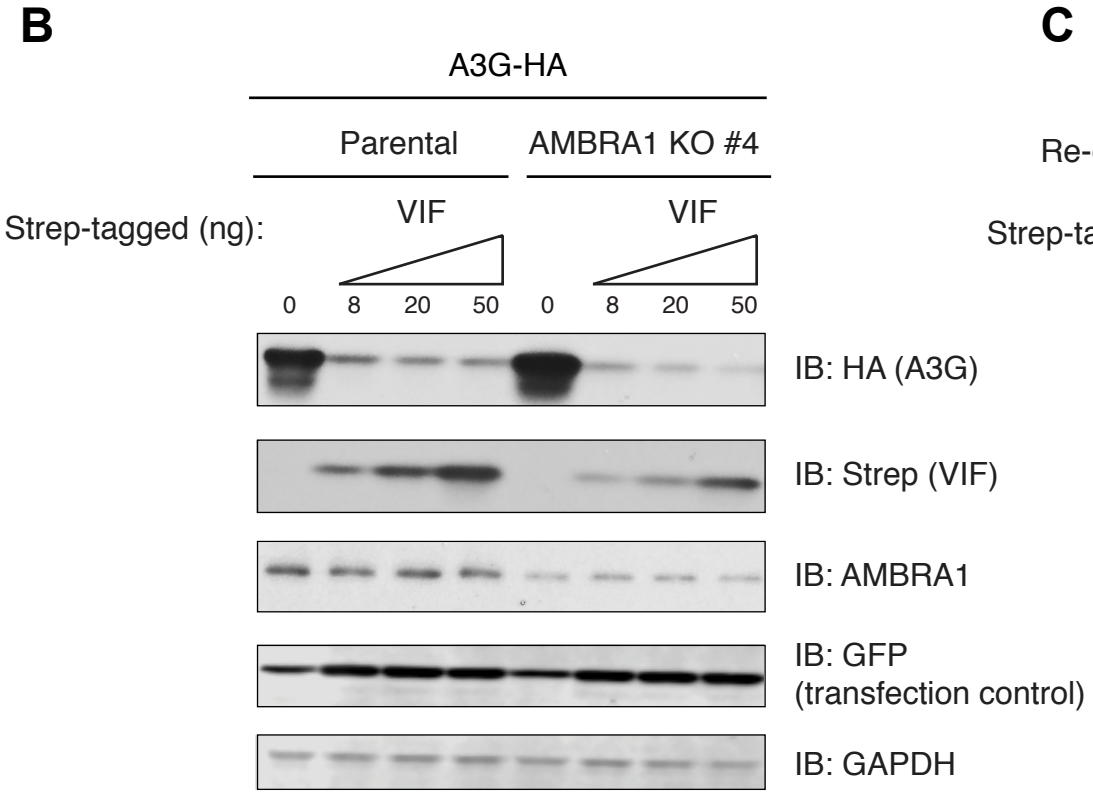

C

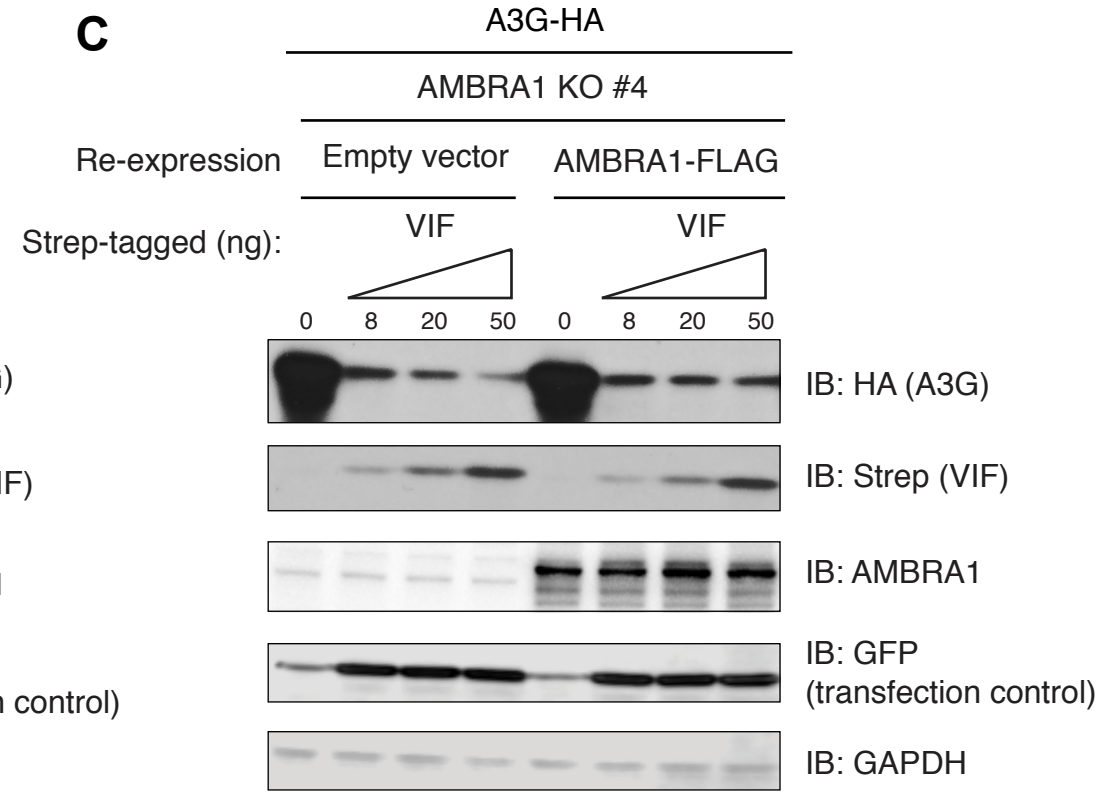

D

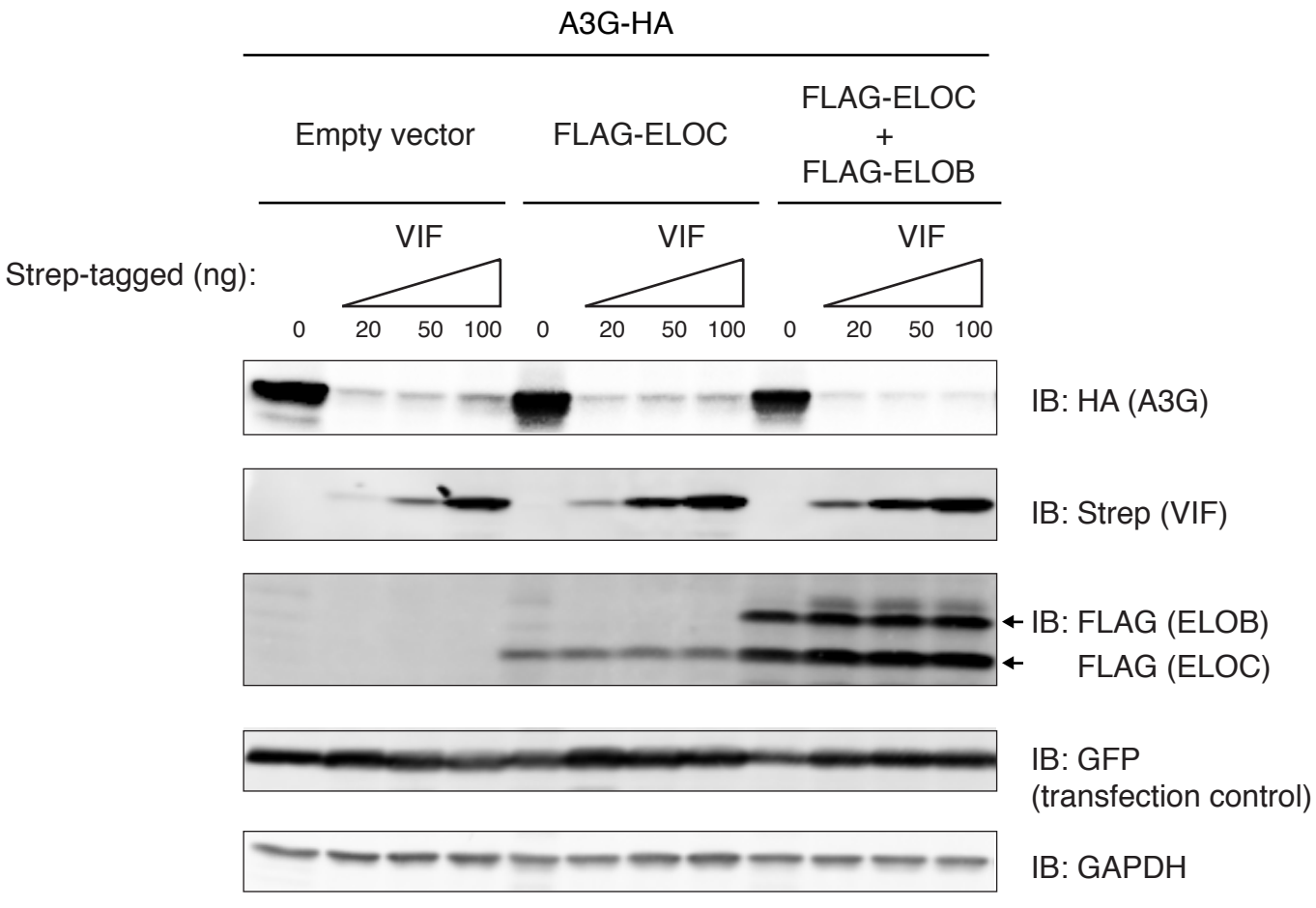

Chen SH et al., Appendix Figure S4

A

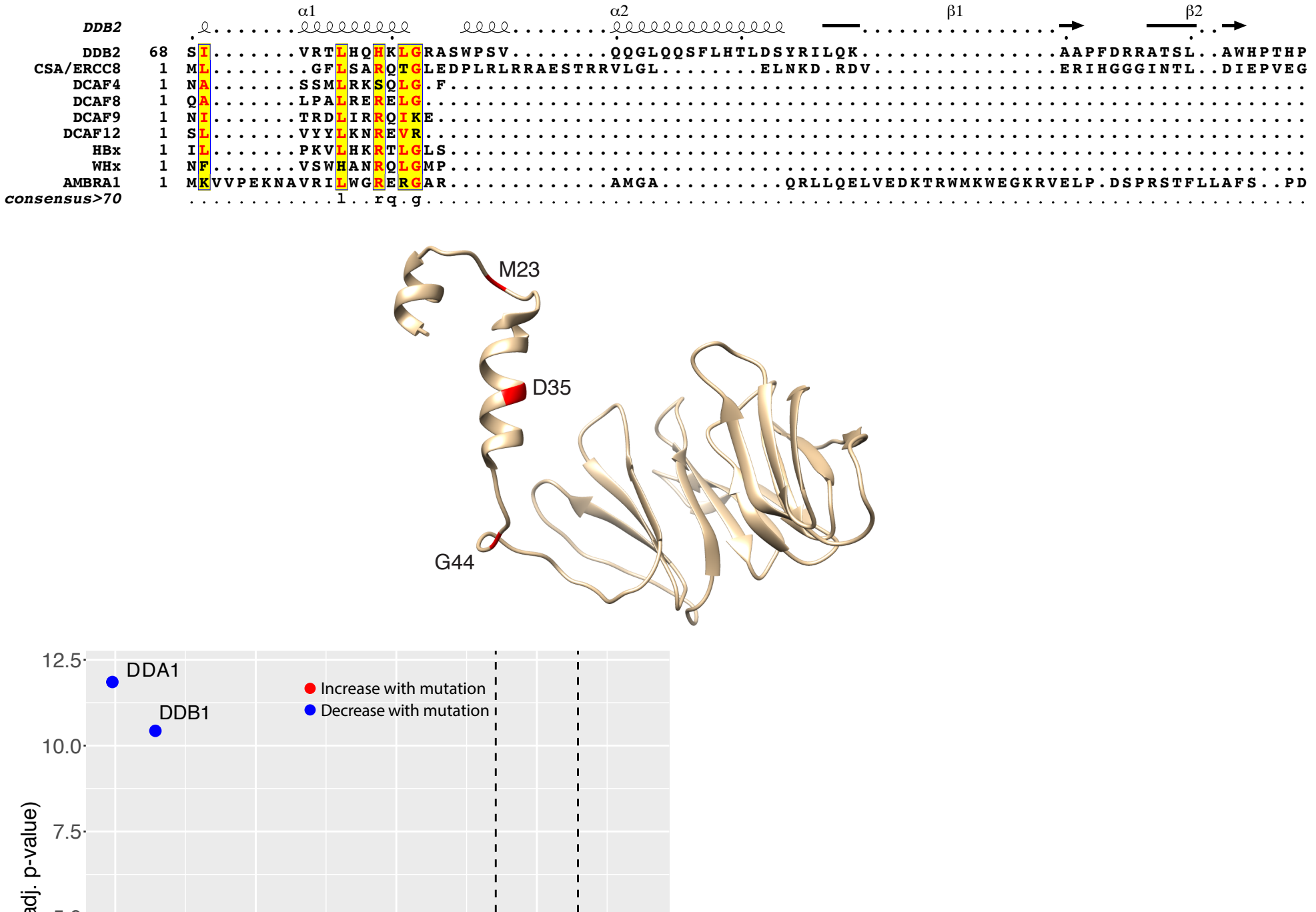

B

C

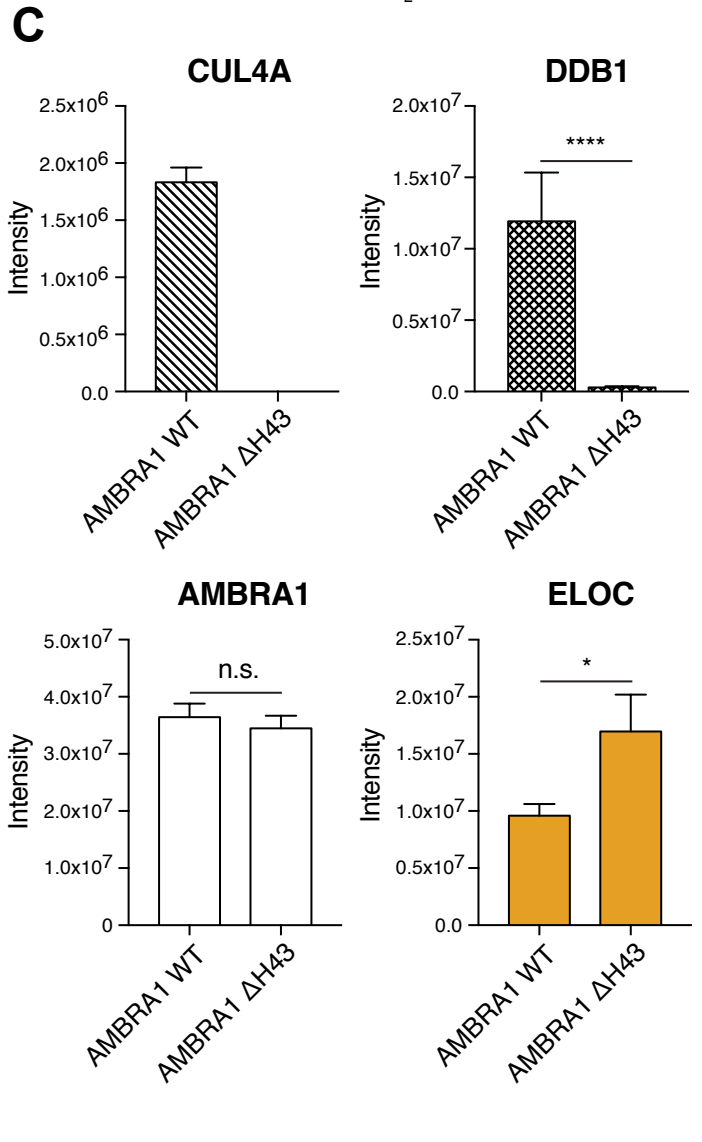

D

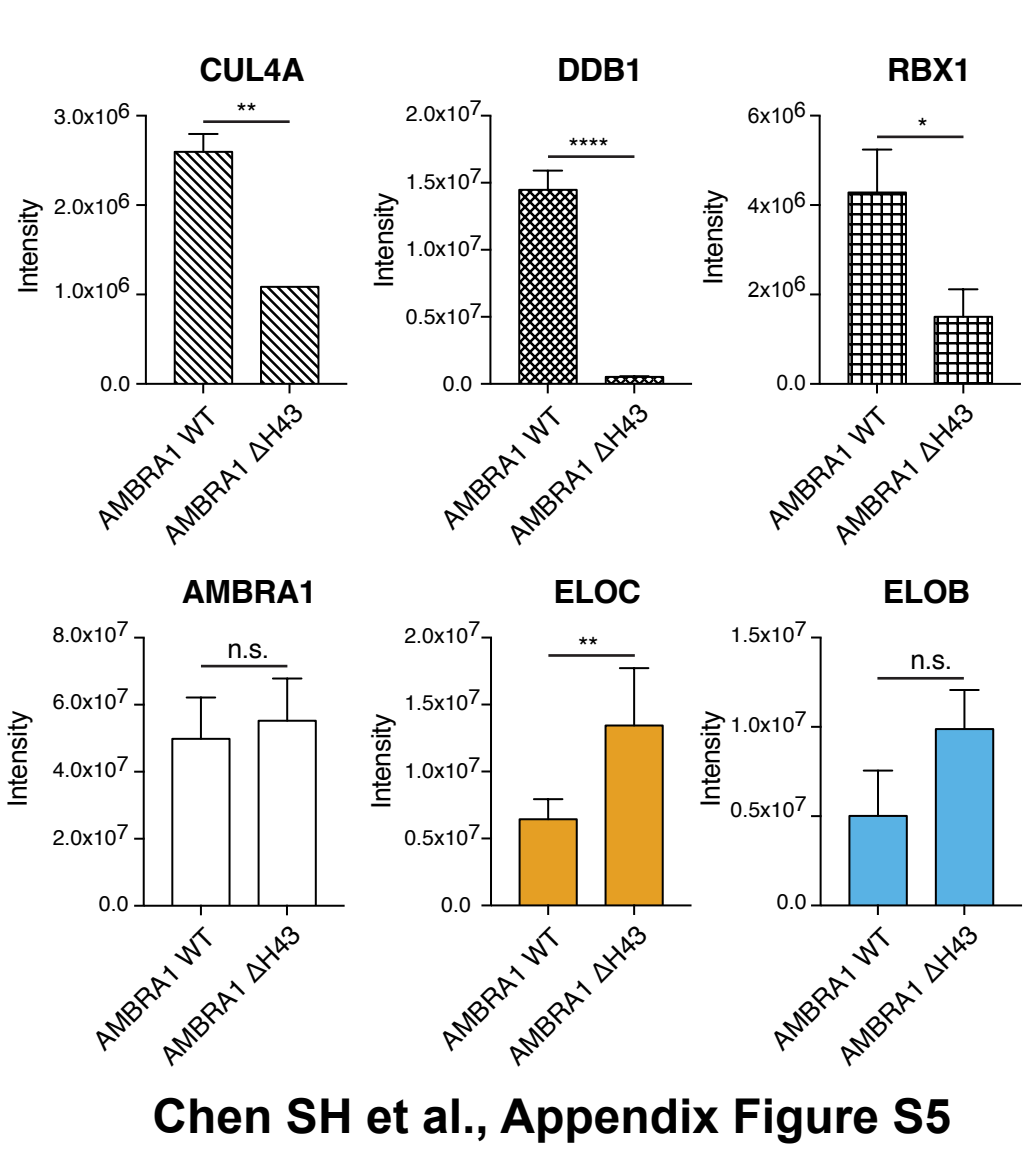

Chen SH et al., Appendix Figure S5

A

```
                                        .                 .
SKP1_HUMAN      1   ..............MPSIKLQSSDGEIFE
ELOC_HUMAN      1   MDGEEKTYGGCEGPDAMYVKLISSDGHEFI
consensus>70        ..................!KL.SSDG..F.

                        .                 .                 .
SKP1_HUMAN     16   VDVEIAKQSVTIKTMLEDLGMDDEGDDDPV
ELOC_HUMAN     31   VKREHALTSGTIKAMLSGPGQFAENETNEV
consensus>70        V..E.A..S.TIK.ML...G...E.#.#.V

                        .                 .                 .
SKP1_HUMAN     46   PLPNVNAAILKKVIQWCTHHKDDPPPPEDD
ELOC_HUMAN     61   NFREIPSHVLSKVCMYFTYKV.......RY
consensus>70        ...#!...!L.KV....T............

                        .                 .                 .
SKP1_HUMAN     76   ENKEKRTDDIPVWDQEFLKVDQGTLFELIL
ELOC_HUMAN     84   TNSSTEIPEFPIAPE.......IA.LELLM
consensus>70        .N......#.P!..#..........EL.$

                        .                 .                 .
SKP1_HUMAN    106   AANYLDIKGLLDVTCKTVANMIKGKTPEEI
ELOC_HUMAN    106   AANFLDC.......................
consensus>70        AAN%LD.......................

                        .                 .                 .
SKP1_HUMAN    136   RKTFNIKNDFTEEEEAQVRKENQWCEEK
ELOC_HUMAN          ............................
consensus>70        ............................
```

B

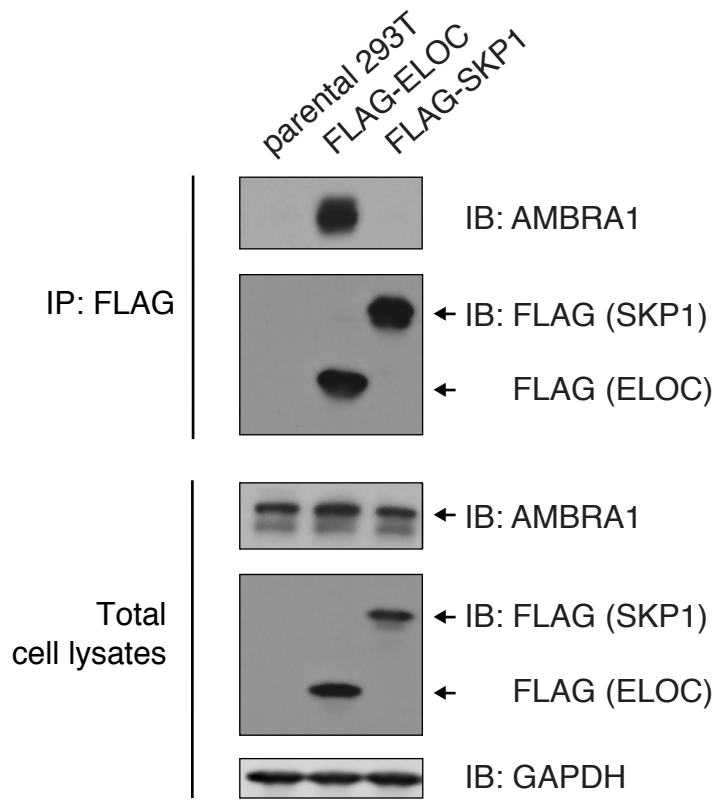

Chen SH et al., Appendix Figure S6

A

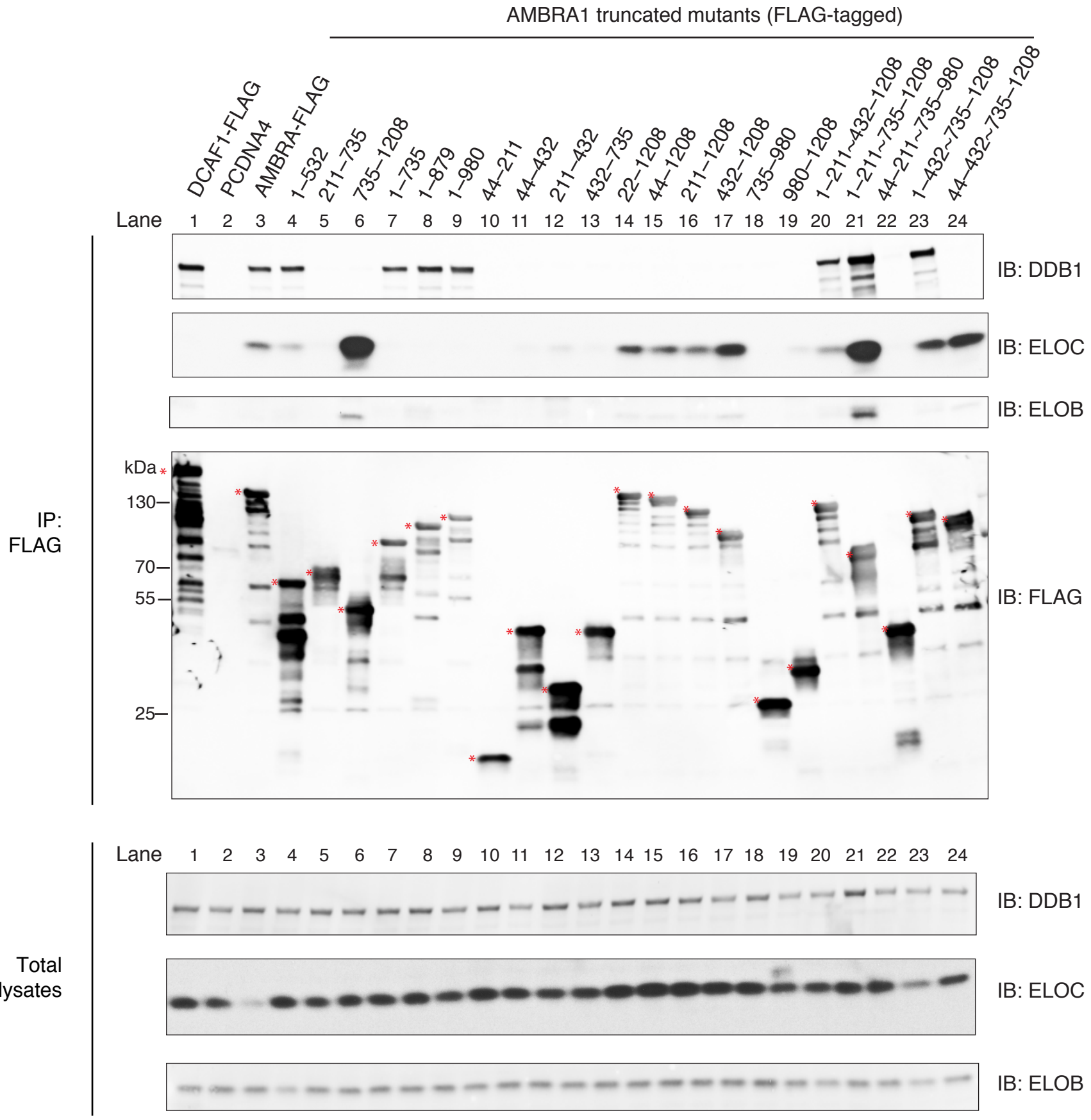

B

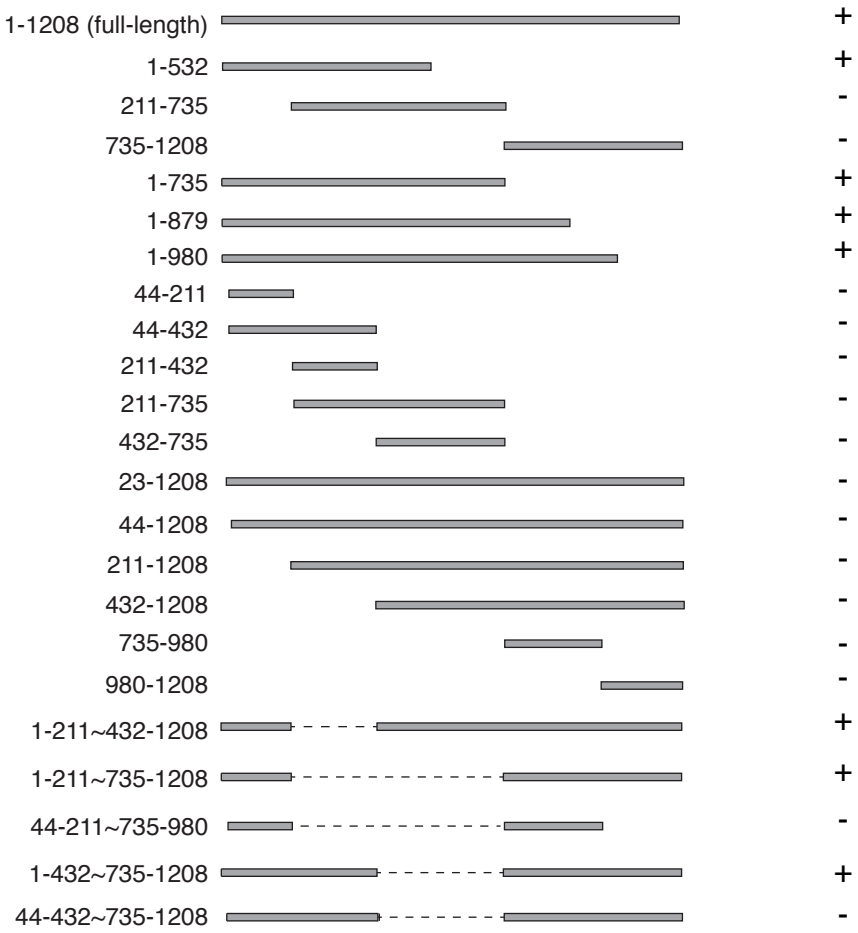

C

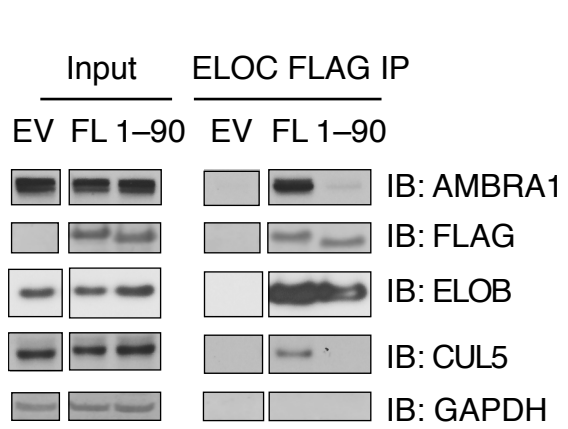

Chen SH et. al, Appendix Figure S7

A

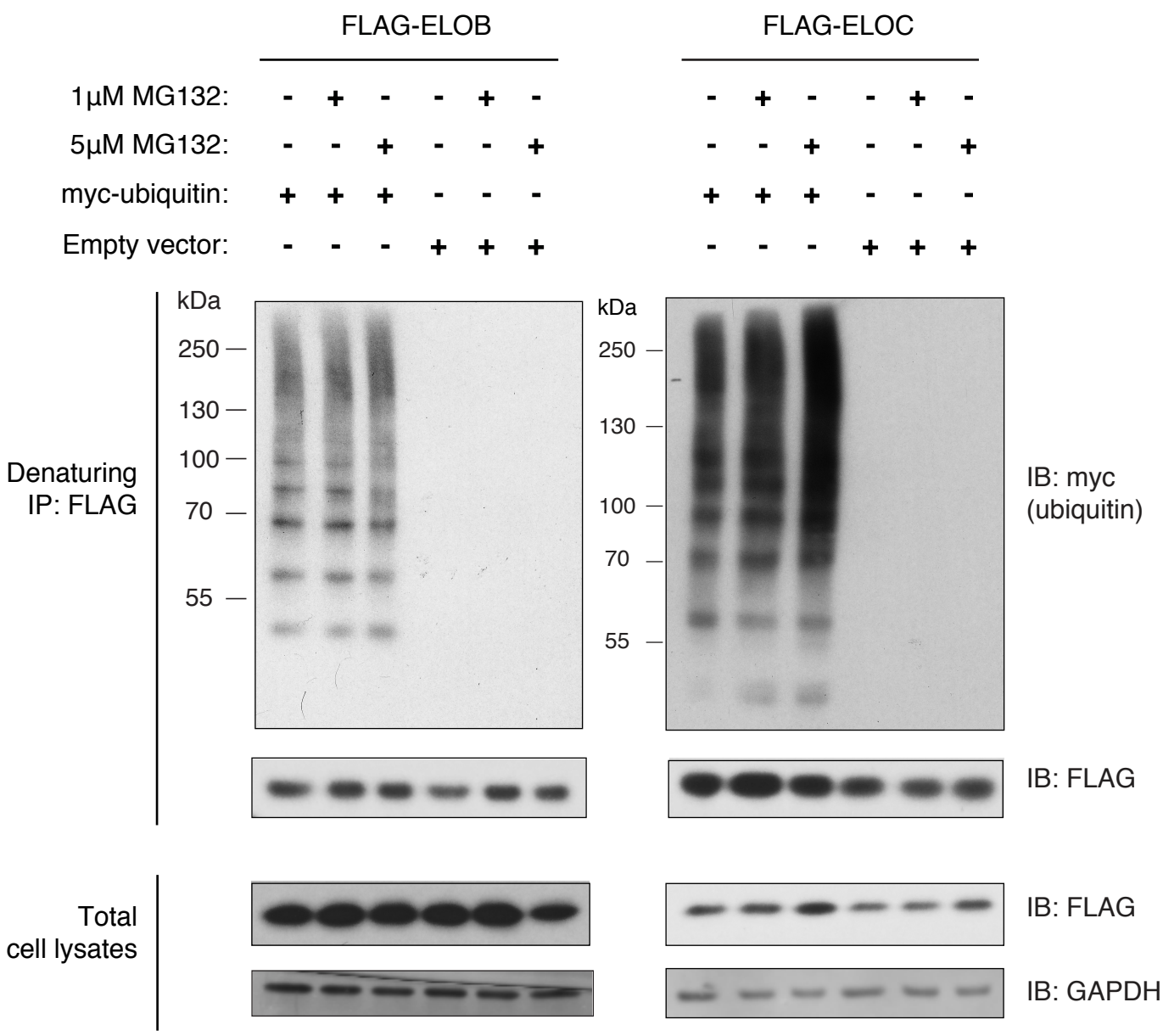

B

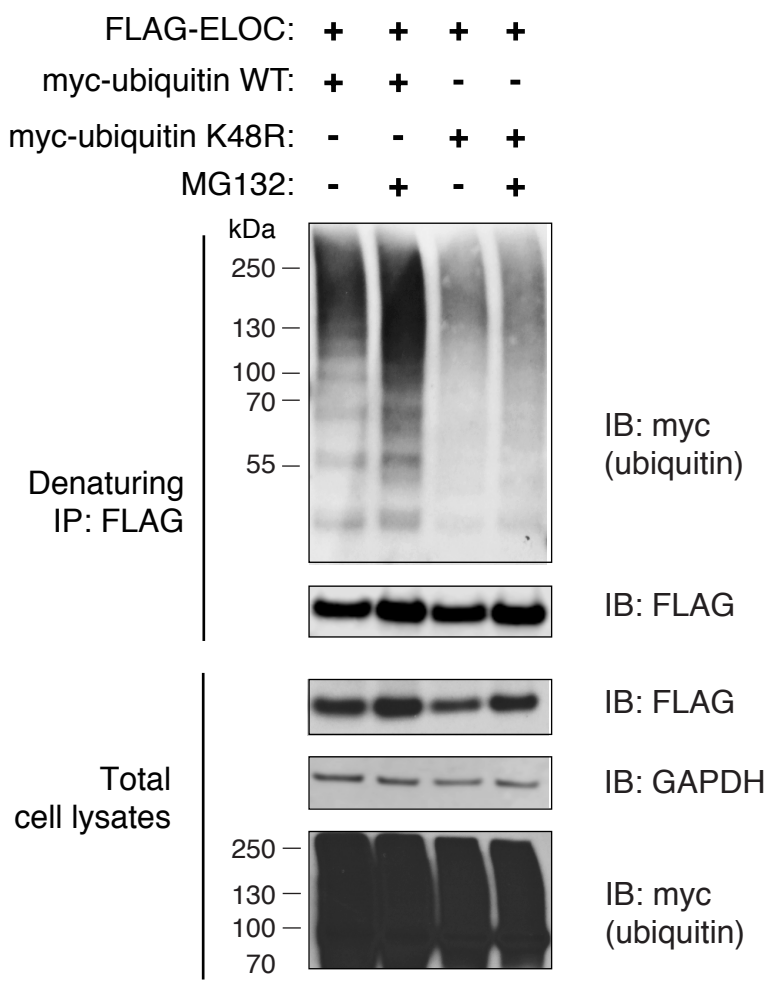

Chen SH et al., Appendix Figure S8

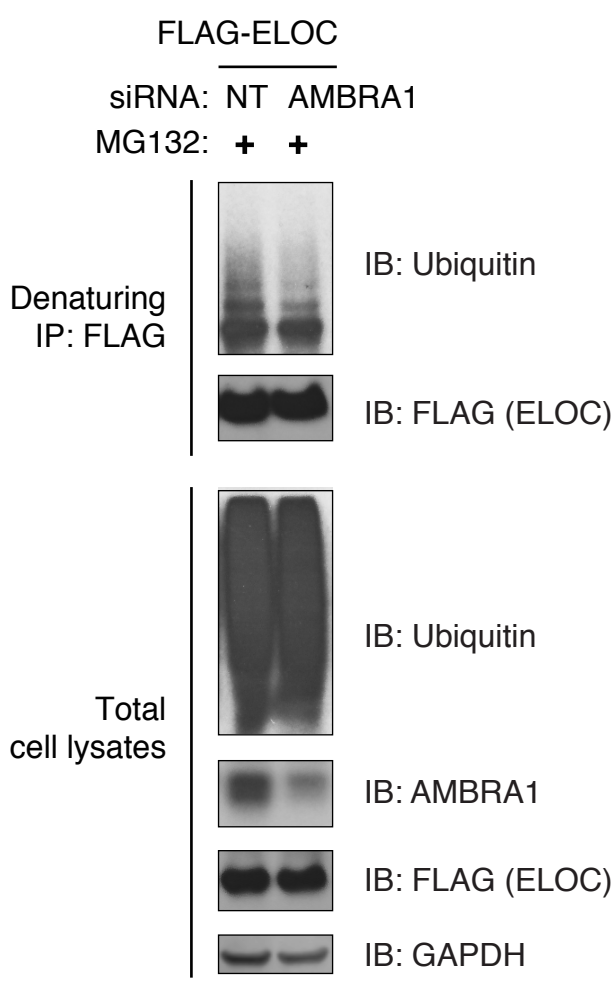

Chen SH et al., Appendix Figure S9

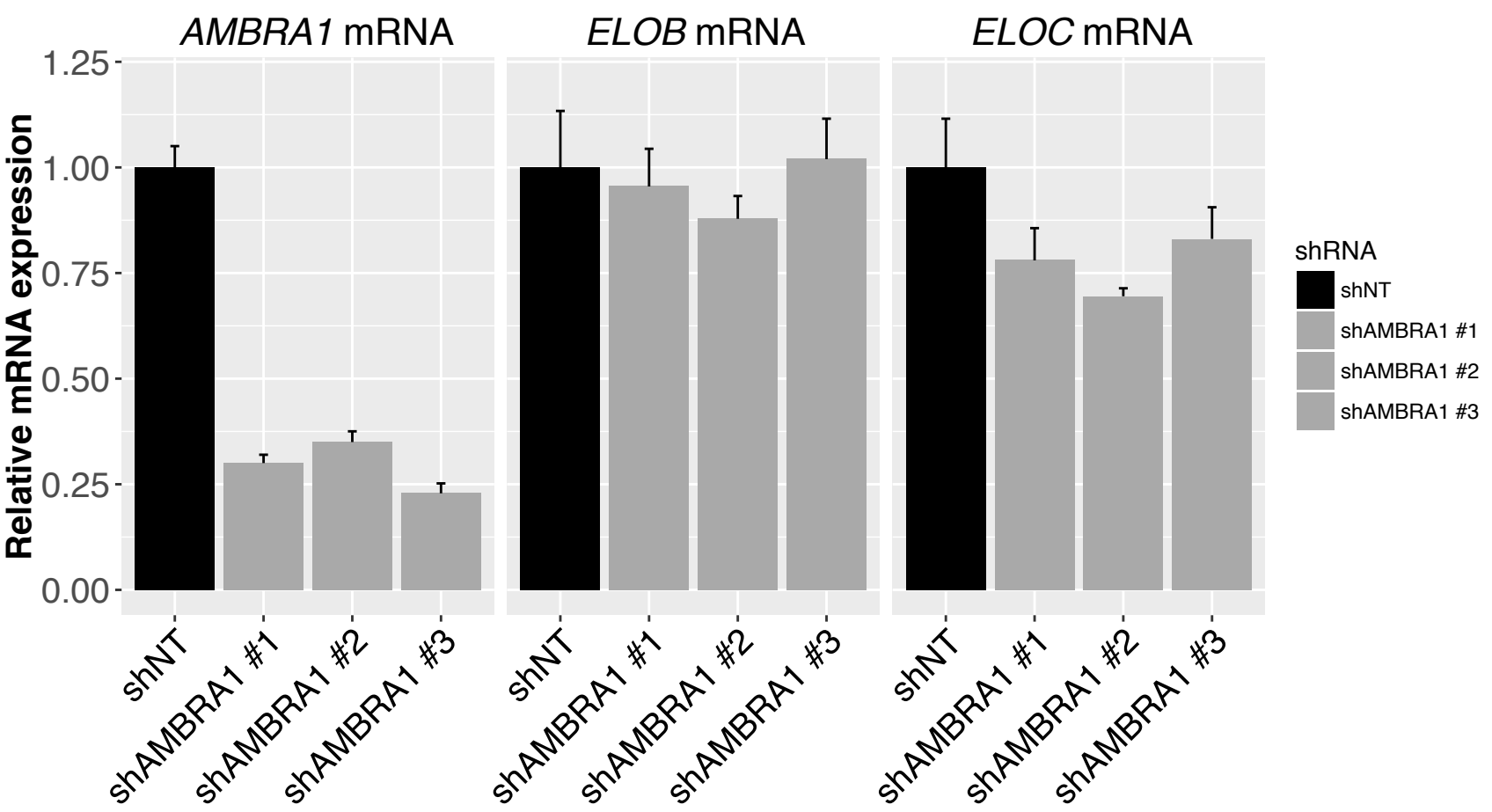

Chen SH et al., Appendix Figure S10

A

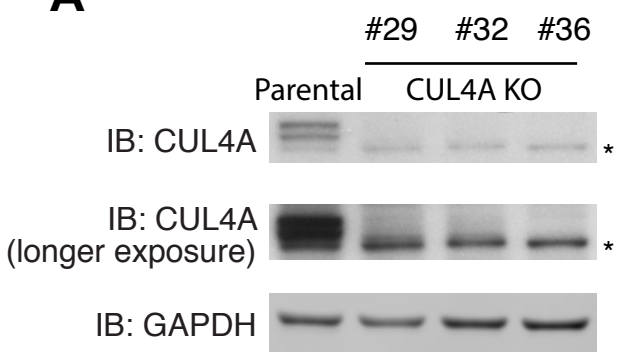

B

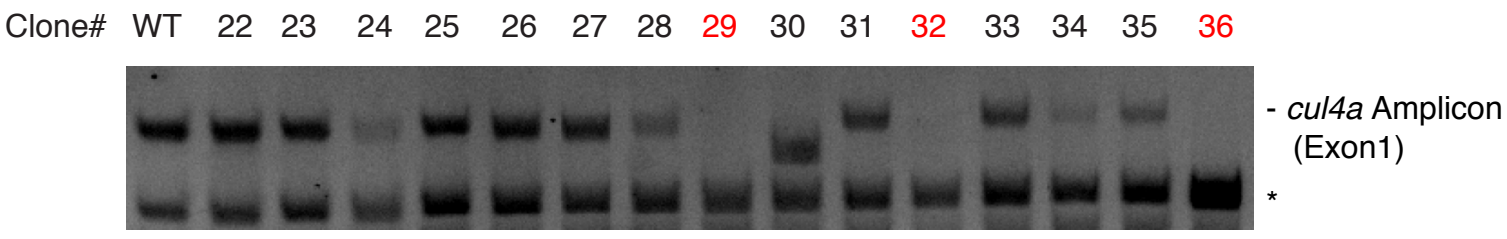

Genomic PCR on genomic locus of *cul4a* on Chromosome 13

C

```
                                                                                PAM
          WT: CTGCCCAGCTATTGGAACACTGTATAACACCAACACACTCGAGTCTTTCAAGACTGCAGATAA
 ATG7 KO#1-1: CTGCCCAGCTATTGGAACACTGTATAACACCA--ACACTCGAGTCTTTCAAGACTGCAGATAA
 ATG7 KO#1-2: CTGCCCAGCTATTGGAACACTGTATAACACCA--ACACTCGAGTCTTTCAAGACTGCAGATAA
 ATG7 KO#1-3: CTGCCCAGCTATTGGAACACTGTATAACACCAACAC----------CAAGACTGCAGATAA

                                                                                PAM
          WT: CTGCCCAGCTATTGGAACACTGTATAACACCAACACACTCGAGTCTTTCAAGACTGCAGATAA
 ATG7 KO#2-1: CTGCCCAGCTATTGGAACACTGTATAA-------AGACTCGAGTCTTTCAAGACTGCAGATAA
 ATG7 KO#2-2: CTGCCCAGCTATTGGAACACTGTATAA-------AGACTCGAGTCTTTCAAGACTGCAGATAA
 ATG7 KO#2-3: CTGCCCAGCTATTGGAA-----------------AGACTCGAGTCTTTCAAGACTGCAGATAA
 ATG7 KO#2-4: CTGCCCAGCTATTGGAA-----------------AGACTCGAGTCTTTCAAGACTGCAGATAA

                                                PAM
          WT: TGTCTCCCCAGAAACAACCACCCCGGAGCCCCCGTCTTCCGCTGCAGTTTCCCCGGGAACAGA
ATG12 KO#2-1: TGTCTCCCCAGAAACAACCACCCCGGAGCCCCCG--TTCCGCTGCAGTTTCCCCGGGAACAGA
ATG12 KO#2-2: TGTCTCCCCAGAAACAACCACCCCGGAGCCCCCG--TTCCGCTGCAGTTTCCCCGGGAACAGA
ATG12 KO#2-3: TGTCTCCCCAGAAACAACCACCCCGGAGCCCCCG--TTCCGCTGCAGTTTCCCCGGGAACAGA
ATG12 KO#2-4: TGTCTCCCCAGAAACAACCACCCCGGAGCCCCCG*TCTTCCGCTGCAGTTTCCCCGGGAACAGA
 & #2-5~#2-7: GCTGCAAAGTTTCTTCAATGGCCACGAGCCATCCCCCAGGAGAACACACAGTTGAAGGGGCACC
              AGCCCCTGCTTCTCTGCTGCAAAGTGAGCCAGATAACCAGGAAAACCCAGATCAATCCTCTGGT
              CAAGGTACAGCAGGAAGTCAAGGCTGCTGCAGAAGTGAACTCACTCAGGAGTTCTGGAGCTGAC
              TCTGGCTAGTCCCAGTCAACAGAGCA

                                                PAM
          WT: TGTCTCCCCAGAAACAACCACCCCGGAGCCCCCGTCTTCCGCTGCAGTTTCCCCGGGAACAGA
ATG12 KO#2-1: TGTCTCCCCAGAAACAACCACCCCGGAGCCCCCGTATCTTCCGCTGCAGTTTCCCCGGGAACAGA
ATG12 KO#2-2: TGTCTCCCCAGAAACAACCACCCCGGAGCCCCCGTATCTTCCGCTGCAGTTTCCCCGGGAACAGA
ATG12 KO#2-3: TGTCTCCCCAGAAACAACCACCCCGGAG----------CCGCTGCAGTTTCCCCGGGAACAGA
ATG12 KO#2-4: TGTCTCCCCAGAAACAACCACCCCGGAG----------CCGCTGCAGTTTCCCCGGGAACAGA
ATG12 KO#2-5: TGTCTCCCCAGAAACAACCACCCCGGAG----------CCGCTGCAGTTTCCCCGGGAACAGA
ATG12 KO#2-6: TGTCTCCCCAGAAACAACCACCCCGGAG----------CCGCTGCAGTTTCCCCGGGAACAGA
```

D

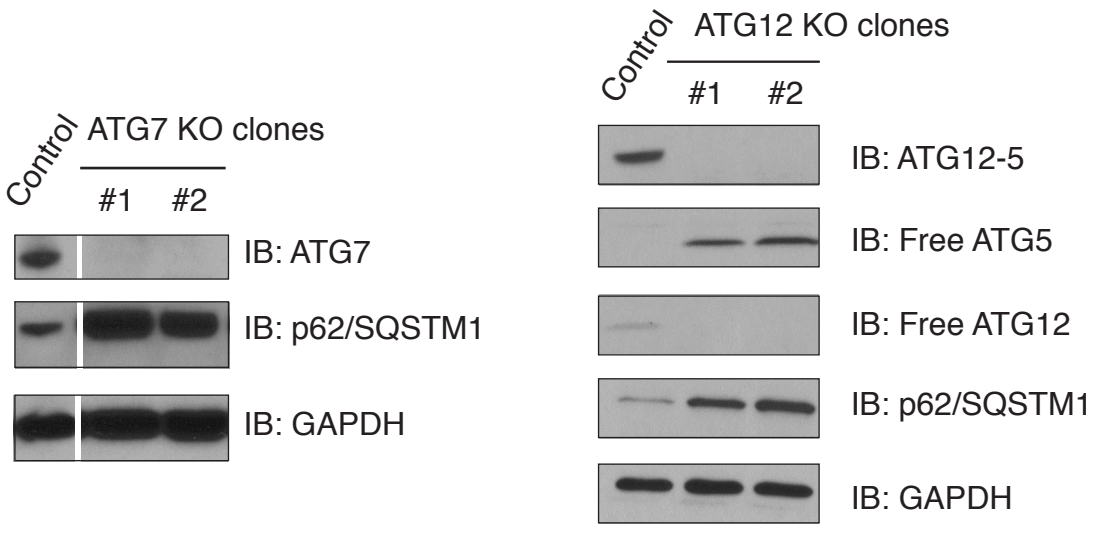

Chen SH et al., Appendix Figure S11

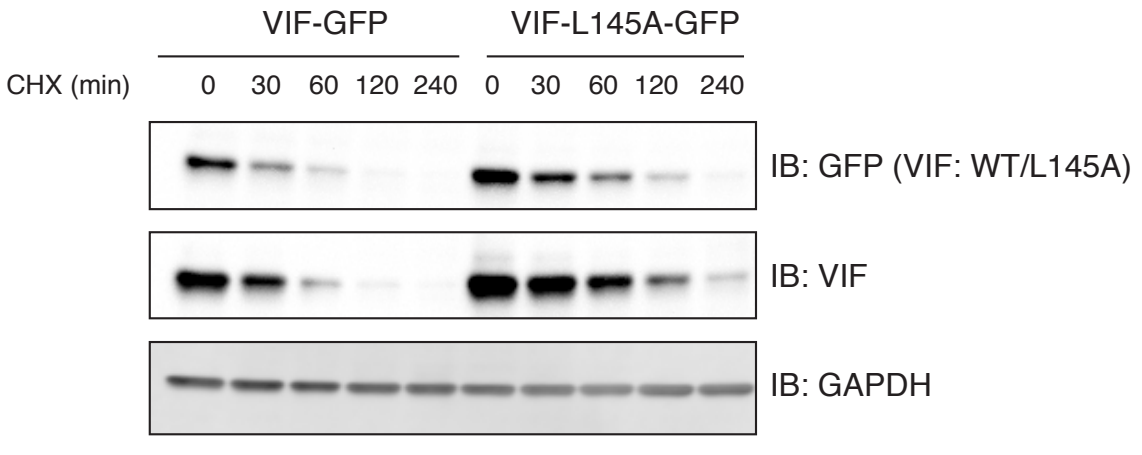

Chen SH et. al, Appendix Figure S12

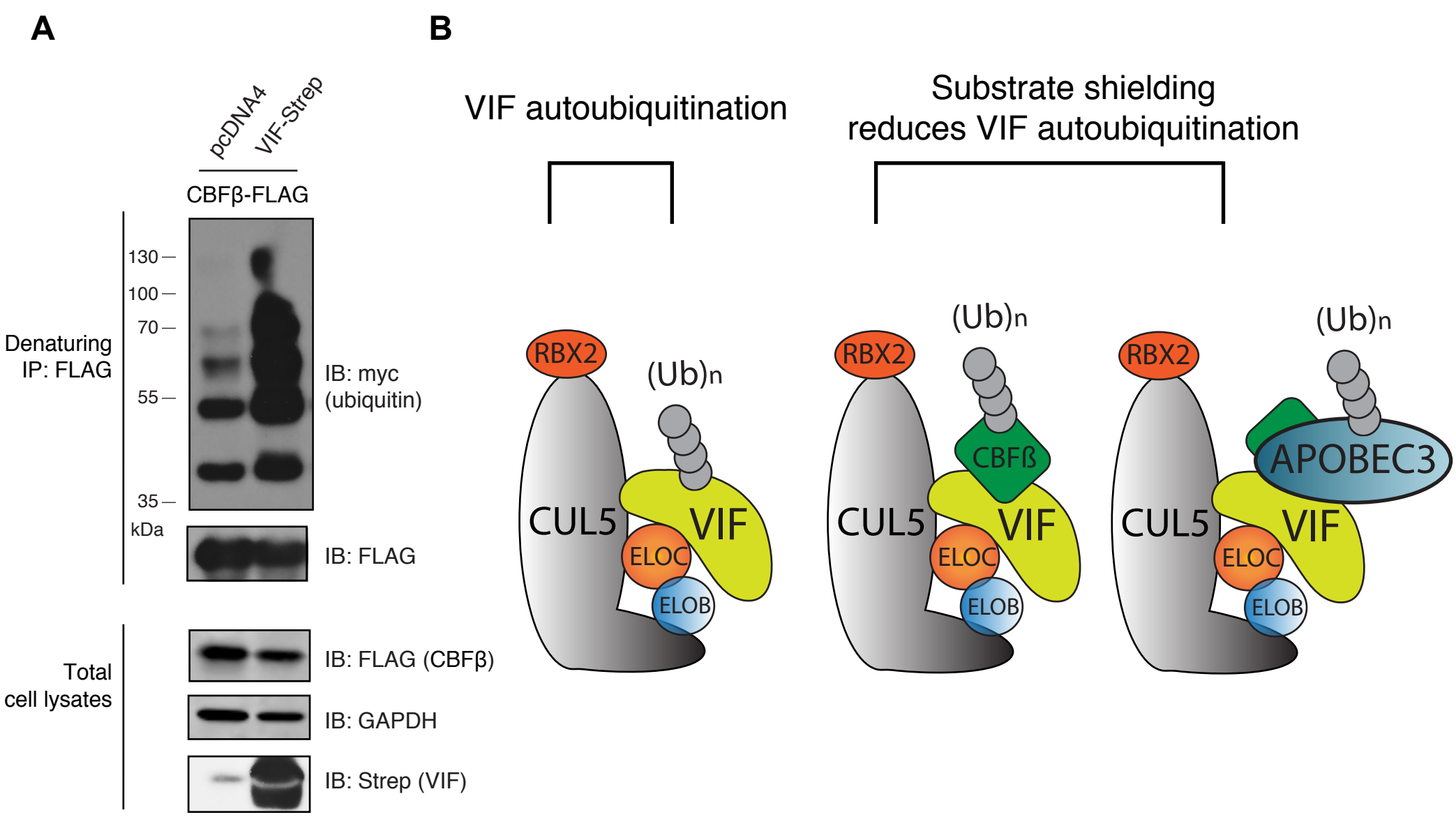

Chen SH et. al, Appendix Figure S13

Appendix Table S1

Key recombinant DNA constructs used in this study

Recombinant DNA	Vector
FLAG-ELOC	pCDH-EF1-MCS-IRES-GFP (SBI)
FLAG-SKP1	pCDH-EF1-MCS-IRES-GFP (SBI)
SOCS3-GFP	Tet-On 3G ZeoR (Clontech)
VIF-GFP	Tet-On 3G ZeoR (Clontech)
VHL-GFP	Tet-On 3G ZeoR (Clontech)
PPIL5-GFP	Tet-On 3G ZeoR (Clontech)
AMBRA1-FLAG	Tet-On 3G ZeoR (Clontech)
AMBRA1 Δ34H-FLAG	Tet-On 3G ZeoR (Clontech)
mCherry-FLAG	pCDH-EF1-MCS-T2A-HygroR (SBI)
AMBRA1-FLAG	pCDH-EF1-MCS-T2A-HygroR (SBI)

Appendix Table S2

Guide RNA sequences used in HIV-1 infection in primary T cells

crRNA	target gene	Guide sequence
AMBRA1-06	AMBRA1	TGGTAGAAGATAAAACCCGG
AMBRA1-07	AMBRA1	AGAATGCTGTCCGGATACTC
AMBRA1-08	AMBRA1	AAGGTAGAGCGTGGACTATC
NT	non-targeting	TCGGATGTAAATTATGCCGT
CXCR4	CXCR4	GAAGCGTGATGACAAAGAGG

Appendix Table S3

The following table includes RNAi-based sequences, sgRNA sequences for CRISPR-Cas9-mediated gene knockout, and primers used to PCR amplify the edited regions.

Sequence-Based Reagents	SOURCE	IDENTIFIER
pLKO.1 Control sh-NT	Sigma-Aldrich	SHC002
pLKO.1 sh-AMBRA1 #1; target GGCTTGGCCTATGGTACTAAC	Sigma-Aldrich	TRCN0000417120
pLKO.1 sh-AMBRA1 #2; target GGCCACTGGGAAAGAATTTAC	Sigma-Aldrich	TRCN0000441636
pLKO.1 sh-AMBRA1 #3; target CCCACTTTCTCCTAGTAACAT	Sigma-Aldrich	TRCN0000167886
si-AMBRA1; UUUGUUAGUACCAUAGGCCAAGCCA	Thermo	pre-designed Stealth#3156
si-ELOB; GCUGUACAAGGAUGACCAAtt	This paper	NA
si-ELOC; CGAACUUCUUAGAUUGUUAtt	This paper	NA
si-CUL5; AGCUGAUUCAGUUAAUAUAtt	This paper	NA
si-SOCS3	Sigma-Aldrich	pre-designed SASI_Hs01_00179195
si-Control	Thermo	Stealth siRNA negative control medium GC, Cat#12935300
si-DDB1 #2	Dharmacon	J-012890-07-0002
si-DDB1 #3	Dharmacon	J-012890-08-0002
si-DDB1 #4	Dharmacon	J-012890-09-0002
si-CUL4B	Dharmacon	J-017965-05-0002
SpCas9-P2A-GFP AMBRA1 sgRNA TGGTAGAAGATAAAACCCGG	This paper	NA
SpCas9-P2A-puro ATG7 ATAGCTGGGCAGCAACGGGC	This paper	NA
SpCas9-P2A-puro ATG12 GAAACTGCAGCGGAAGACGG	This paper	NA
CUL4A sgRNA CGGCGGTTCCGGCCCAGCC	This paper	NA
AMBRA1 genotyping forward primer tagaactagtggatccCTTCTCGTTGCAGAAGTCGT	This paper	NA
AMBRA1 genotyping reverse primer gcttgatatcgaattcCAGATATGTCAACTCTCCCACACA	This paper	NA
ATG7 genotyping forward primer caccg TGGGGGACAGTAGAACAGCA	This paper	NA
ATG7 genotyping reverse primer aaac CCTGGATGTCCTCTCCCTGA	This paper	NA
ATG12 genotyping forward primer caccgAGCCGGGAACACCAAGTTT	This paper	NA
ATG12 genotyping reverse primer aaacGTGGCAGCCAAGTATCAGGC	This paper	NA
CUL4A editing site forward primer GAGGGGGTGTCCGAATCTCT	This paper	NA
CUL4A editing site reverse primer GCTCCTCGAGATGGTCCACT	This paper	NA

Appendix Table S4

Antibodies used in this study

Antibodies	SOURCE	IDENTIFIER
Rabbit polyclonal anti-AMBRA1	EMD-Millipore	ABC131
Rabbit polyclonal anti-AMBRA1	Bethyl	A302
Mouse monoclonal anti-ELOC	BD Biosciences	#610761
Rabbit monoclonal anti-ELOB	Abcam	ab154854
Rabbit monoclonal anti-CUL4A	Abcam	ab92554
Rabbit polyclonal anti-CUL4B	Sigma-Aldrich	SAB2107673
Mouse monoclonal anti-DDB1	Thermo Fisher	#39-9901
Mouse monoclonal anti-STAT3	Cell Signaling Technology	#9139
Rabbit monoclonal anti-Phospho-STAT3 (Tyr705)	Cell Signaling Technology	#9145
Rabbit polyclonal anti-SOCS3	Cell Signaling Technology	#2932
Rabbit polyclonal anti-GAPDH	Cell Signaling Technology	#2118
Mouse monoclonal anti-GAPDH	Thermo Fisher	MA5-15738
Rabbit polyclonal anti-GFP	Abcam	ab6556
Mouse monoclonal anti-GFP	Santa Cruz	sc9996
Mouse monoclonal anti-HA	Cell Signaling Technology	#2367
Rabbit polyclonal anti-Myc	Abcam	ab9106
Guinea pig polyclonal anti-p62/SQSTM1	Progen	GP62-C
Mouse monoclonal anti-p62/SQSTM1	Novus	#2C11
Rabbit polyclonal anti-LC3	EMD-Millipore	ABC232
Goat polyclonal anti-ATG7	Santa Cruz	sc8668
Rabbit polyclonal anti-ATG12	Cell Signaling Technology	#4180